Available online at www.sciencedirect.com
SCIENCE DIRECT®
International Journal of Heat and Mass Transfer 49 (2006) 1876–1884
International Journal of HEAT and MASS TRANSFER
www.elsevier.com/locate/ijhmt

Crystallisation of undercooled aqueous solutions: Experimental study of free dendritic growth in cylindrical geometry

V. Ayel [a,*], O. Lottin [b], M. Faucheux [c], D. Sallier [c], H. Peerhossaini [c]

[a] Laboratoire d'Etude Thermique, CNRS UMR 6608, BP 40109, 1, Avenue Clément Ader, 86961 Futuroscope Chasseneuil Cedex, France
[b] Laboratoire d'Energétique et de Mécanique Théorique et Appliquée, UMR 7563 CNRS-INPL, Université Henri Poincaré, BP 160, 2 Avenue de la Forêt de Haye, 54504 Vandoeuvre-lès-Nancy, France
[c] Laboratoire de Thermocinétique, CNRS UMR 6607, Ecole Polytechnique de l'Université de Nantes, BP 50609, 44306 Nantes, France

Received 2 March 2005; received in revised form 22 August 2005
Available online 10 February 2006

Abstract

This paper reports a study of crystallisation kinetics in small volumes of undercooled water–MPG (monopropylene glycol) mixture. The experimental cell is a vertical cylinder (height 5 mm, diameter $2r_e = 7.5$ mm); its bottom section is closed by a Plexiglas disc that transmits light from the lower part of the cylinder to a high-speed digital camera. Photographic recordings allow the determination of the crystal growth rate. When the antifreeze mass fraction is below 25 wt%, crystallisation is clearly divided into two stages: the growth of dendritic crystals in the undercooled solution followed by the passage of the interdendritic solidification front. Dendrite growth induces a sudden temperature increase in the mixture, while the passage of the interdendritic solidification front determines the time at which sensible heat effects again predominate. The results show that the dendrite growth rate is an increasing function of the degree of undercooling and a decreasing function of the antifreeze mass fraction.

Keywords: Dendrites; Freezing; Undercooling; Solidification; Phase transition; Aqueous solution; Antifreeze

1. Introduction

Water–antifreeze mixtures are widely used as secondary refrigerants in refrigeration and air-conditioning systems, thus minimizing the quantity of environmentally harmful primary refrigerants and confining them to a restricted area. Monopropylene glycol (MPG) is one of the most commonly used antifreezes, either in liquid solution or in two-phase liquid–ice mixture as a phase-change secondary refrigerant. This latter technique raises the possibility of exploiting the latent heat of ice to increase the apparent heat capacity of the mixture, thus improving the overall efficiency of the system. Understanding the phenomena involved during the process of crystallisation of these aqueous solutions is useful in preventing the bursting of pipes [1] and in controlling ice production in heat exchangers, an issue particularly relevant to systems that produce ice starting from an undercooled solution [2].

The objectives of this paper are to synthesise information of the literature about the freezing mechanisms of water–antifreeze mixtures and to complement them with an experimental study of crystallisation kinetics in undercooled water–MPG mixtures. This study is restricted to small volume samples in a cylindrical geometry and we focus on the dependence of dendrite growth rate on undercooling degree and on antifreeze mass fraction.

Section 2 gives a brief outline of the physics of crystallisation of undercooled solutions. The experimental set-up is described in Section 3 and the results obtained for the global solidification process are detailed in Section 4. The dependence of dendrite growth rate on undercooling degree and on antifreeze mass fraction is discussed in Section 5, and conclusions are given in Section 6.

* Corresponding author. Tel.: +33 5 4949 8125; fax: +33 5 4949 8101.
E-mail address: vincent.ayel@let.ensma.fr (V. Ayel).

0017-9310/$ - see front matter © 2005 Elsevier Ltd. All rights reserved.
doi:10.1016/j.ijheatmasstransfer.2005.10.036

Nomenclature

c_p	mass heat capacity (J °C^{-1} kg^{-1})
L_f	latent heat of solidification (J kg^{-1})
r	radius (m)
t	time (s)
T	temperature (°C)
x	mass fraction (kg kg^{-1})
y	relative position (%)
ΔT	degree of undercooling (°C)

Greek symbol

v	velocity of dendrites growth (mm s^{-1})

Subscripts

a	antifreeze
c	beginning of crystallisation
e	external (wall)
eq	thermodynamic equilibrium
f	freezing
i	initial
l	liquid
r	relative
s	solid

2. Freezing mechanism of undercooled solutions

Experimental and theoretical work on solidification since the 1950s have been analysed and summarised by Müller-Krumbhaar and Kurz [3], Papon et al. [4] or Huppert [5]. Crystallisation is a phase-transition phenomenon, governed by the laws of thermodynamics, heat transfer, and kinetics, that proceeds in two stages: nucleation and crystalline growth. Nucleation is the formation of microstructures of a new solid phase in the liquid one. Crystalline growth follows by the addition of molecules or particles on the interface separating the liquid and the most recently formed crystals. Thus, diffusion in the liquid phase of the solidifying compound is one of the most significant phenomena involved in crystallisation. Heat diffusion also has a very important role because crystallisation calls into play the latent heat of solidification. Finally, particle aggregation at the liquid–solid interface depends on interfacial tension [4].

Considering solidification of an initially liquid aqueous solution, one can obtain the curves for temperature vs. time shown on the right-hand side of Fig. 1 (for a 15 wt% monopropylene glycol–water mixture). The graph on the left-hand side of Fig. 1 represents the evolution of temperature and composition of the liquid and solid phases in the MPG–water phase diagram, assuming that they are in thermodynamic equilibrium. Note that, considering the small temperature range we are interested in, the solute always remains in liquid phase and the solidus is assumed strictly vertical [5]. The liquid–solid transition can be divided into four stages [1,6]:

- Between a and b: sensible cooling stage during which the mixture remains liquid in a thermodynamically stable state; the temperature is above that of solid–liquid equilibrium $T_{eq}(x_{a,i})$ [1].
- Between b and c: sensible cooling stage during which the mixture is undercooled in a thermodynamically unstable state described as metastable. The temperature is below the solid–liquid equilibrium temperature $T_{eq}(x_{a,i})$.
- Between c and d: steep temperature increase between T_c and the maximum temperature of crystallisation T_{mc}. This temperature increase characterises the return to thermodynamic equilibrium accompanied by latent heat release associated with ice formation. As for most of aqueous solutions, the vertical solidus in the MPG–water phase diagram (Fig. 1) implies that the solid phase is exclusively made of ice crystals [1,5]. Note that, due to the increase in solute concentration in the residual liquid (linked to the appearance of ice), the maximum temperature of crystallisation of binary mixtures is necessarily below the solid–liquid equilibrium temperature of the initial mixture $T_{eq}(x_{a,i})$ [7].
- Between d and e: the mixture is still cooled through the vessel walls. The temperature variations are small due to the high apparent heat capacity of the solidifying solution. Then (after point e), the mixture is almost completely solidified and sensible effects again predominate: the apparent heat capacity is low and the temperature decrease is steep [8].

2.1. Undercooling

Most liquids crystallise only if they pass through an undercooled state [4], which corresponds to the persistence of liquid, free of solid crystals, at temperatures below the transition point T_{eq} defined by the liquidus (between b and c in Fig. 1). In the undercooled state, some nuclei of the solid phase appear in the liquid, but they are not large enough to induce crystal growth in the entire system. Once a nucleus reaches the critical size, crystallisation occurs at a temperature T_c below T_{eq}. The degree of undercooling is defined as the difference between these two temperatures (1)

$$\Delta T = T_{eq} - T_c \tag{1}$$

Values of T_c are controlled by stochastic phenomena and depend on sample volume, presence of foreign bodies, thermal history and cooling rate [9,10].

The influence of solutes on aqueous mixture undercooling is not clearly known. We observe that liquid antifreezes like MPG (monopropylene glycol) or MEG (monoethylene glycol) can prevent nucleation, probably by limiting inter-

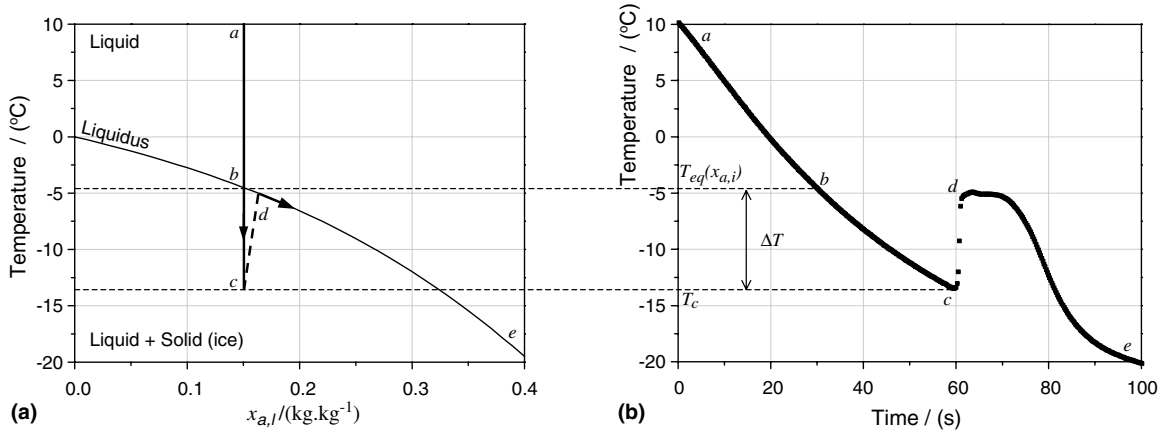

Fig. 1. Cooling and crystallisation of a small volume of a 15 wt% monopropylene glycol (MPG) solution ($T_{eq} = -4.49$ °C): (a) temperature–composition evolutions in phase diagram (vertical solidus not represented); (b) evolution of temperature measured in the centre of the cell.

actions between water molecules: previous experimental data [11] show that the degree of undercooling increases with antifreeze concentration. However, according to Akyurt et al. [1], the presence of solute can promote crystallisation, so that the degree of undercooling decreases with increasing solute concentration. This is in contradiction with our experimental results [11] but the work of Akyurt et al. was carried out in conditions very different from ours and rather concerns the freezing of water in the presence of a nucleating agent. On the other hand, our results suggest that MEG or MPG do not act as nucleating agents. One can add that the higher viscosity of most liquid antifreeze–water mixtures than pure water limits the diffusion of water molecules.

Note that Wilson et al. [12] report that in biological systems, the presence of solutes has no measurable influence on the degree of undercooling since this latter is highly stochastic.

2.2. Physics of crystallisation in aqueous solutions and dendrite geometry

Crystallisation of an undercooled liquid leads to a dendritic ice structure [13] characteristic of a mushy region where liquid and solid phases coexist at thermodynamic equilibrium [5]. The mushy region separating pure liquid from dense crystals can be a few μm to a few cm thick.

In most of the cases, the crystal growth is fast enough (for example, less than 2 s in Fig. 1) so that the latent heat release overcomes the heat extraction rate imposed by the cooling [14]. Once started, crystal growth takes place until all the energy stored by sensible cooling (between T_{eq} and T_c) is consumed [15].

Dendrites develop in the direction of the negative temperature gradient. The driving force controlling their growth is the temperature difference $T_{eq}(x_{a,l}) - T_l$, where $x_{a,l}$ and T_l are, respectively, the antifreeze concentration and the temperature of the liquid phase ahead of the ice front. $T_{eq}(x_{a,l}) - T_l$ can be interpreted as the local value of the degree of undercooling ΔT (1).

According to Papon et al. [4], in pure liquids, the complexity of the dendritic network is originated by capillary forces and reinforced by thermal phenomena. The solid–liquid interface is initially undulated due to capillary forces [16,17]: during their growth, crystals release latent heat of solidification that is more easily dissipated at the tip than in the hollows [16,17]; thus, crystallisation is slowed down in the hollows and accelerated at the tip, which is at the origin of a privileged direction of crystal growth giving birth to the main branches. For similar reasons, secondary branches can appear, perpendicular to the first ones [3]. This is not always the case in pure water where the dendrites can resemble needle crystals for strong undercooling [18]. The Gibbs–Thomson free energy has a major influence on the interface structure [1,3], although its order of magnitude is small compared to the sensible heat and latent heat affecting the global crystallisation process.

In aqueous solutions, many phenomena can be observed in addition to those already discussed. According to Teraoka et al. [18,19], who studied dendritic growth in water–MEG mixtures, the more antifreeze there is in the mixture, the thinner the main and secondary branches are. According to Huppert [5], the slow solutal diffusion influences greatly the shape of the liquid–solid interface, this latter becoming highly irregular. As a consequence, solution of higher concentration remains entrapped between the dendrites, which entails a decrease in the driving force for crystal growth $T_{eq}(x_{a,l}) - T_l$ [20] and the multiplication of secondary branches [18,19].

Therefore, crystal growth in aqueous solution is also controlled by solute concentration in the mushy region and in the liquid immediately ahead of the liquid–solid interface [5,7,14,21,22]. The relative importance of these last parameters (compared to thermal diffusion and to capillary forces) is not clearly known. Loginova et al. [14], studying numerically the solidification of binary alloys, found that the development of dendrite patterns was mainly governed by solute diffusion. However, the physical properties of Ni–Cu alloys being significantly different from those of aqueous solutions, these results should not

be generalised: the limiting phenomenon is probably highly dependent on the materials.

In summary, one can say that dendrite shape is a function of material properties, solutal composition, temperature gradient in the undercooled liquid and surface tension, but that the relative influence of these parameters has not yet been clearly established.

2.3. Amount of ice created

Crystallisation of an undercooled liquid is accompanied by the release of latent heat of solidification. According to Pruppacher [23], heat transfer is negligible during dendritic growth in a water drop. This can also be the case in small samples of low-concentration water–antifreeze mixtures, as indicated in Fig. 1: the time between points c and d (corresponding to dendritic growth) is very small compared to the total solidification time (between points c and e). By considering the dendritic growth as isenthalpic and the heat capacity of undercooled liquid as constant (equal to the liquid heat capacity at 0 °C), one can evaluate the amount of ice created during dendrite growth (2)

$$x_s = \frac{h_l(T_c) - h_l(T_{eq})}{h_s(T_c) - h_l(T_{eq})} \approx \frac{c_{p,l}(T_{eq} - T_c)}{L_f} \approx \Delta T/80 \text{ with water} \tag{2}$$

Eq. (2) is valid for pure liquid, but cannot be used with aqueous mixtures since the maximal temperature of crystallisation reached after dendritic growth is not equal to the equilibrium temperature used in defining the degree of undercooling (1) [11]. As shown by Eq. (2), the quantity of ice x_s present in the mixture after dendritic growth is directly proportional to the degree of undercooling ΔT.

2.4. Kinetics of dendritic growth

It is generally accepted that dendritic growth rate increases with the local undercooling $T_{eq}(x_{a,l}) - T_l$ [3,13,16,18,23,24]. Knight [13] and Müller-Krumbhaar and Kurz [3] use the non-dimensional temperature τ (3)

$$\tau = \frac{T_{eq}(x_{a,l}) - T_l}{\frac{L_f}{c_p}} \tag{3}$$

Note that the expression for τ is strictly the same as that for mass fraction of crystallised water (2). One can conclude that the crystal growth rate depends mostly on thermal phenomena occurring at the solid–liquid interface.

In aqueous solutions, the presence of the solute seems to slow crystal growth [23]; three possible explanations can be put forward:

- The solid–liquid equilibrium temperature decreases with increasing ice fraction (i.e. increasing solute concentration in the residual liquid), thus limiting the driving force $T_{eq}(x_{a,l}) - T_l$ or τ.
- It is highly probable that mass diffusion also limits the crystal growth velocity, but to an extent which is difficult to evaluate.
- In the particular case of MEG and MPG, the viscosity of solutions is higher than that of pure water and increases with antifreeze concentration: this can slow down particles movement towards the growing crystals.

Note that according to Teraoka et al. [18], the dendrites grow faster than in pure water in MEG solution of low concentration (below 1 wt%) because of their smaller radius.

3. Experimental set-up and procedure

The kinetics of dendritic growth can be studied experimentally by analyzing photographs of growing dendrites, particularly for water and many aqueous solutions, which transparency allows the visualisation of crystal growth by photographic analysis [18,19,25]. Müller-Krumbhaar and Kurz [3] described different experimental apparatuses for measuring crystal growth rates. There are two main cases: free growth in an undercooled liquid and directional growth in a sample in which temperature gradients or heat fluxes are controlled.

In free growth studies, crystallisation is governed by nucleation in the undercooled liquid. Therefore, the vessel walls are as little catalytic as possible. Crystals grow while the liquid–solid interface temperature remains above that of the surrounding liquid (i.e., the temperature gradient from solid to liquid is negative). The crystal growth rate v and dendrites size and shape are measured as functions of the undercooling degree ΔT. Crystallisation can be started artificially or not. Thermal and solutal convection are generally avoided in order to compare experimental results with theories of mass diffusion-controlled growth.

In directional growth studies, the first crystal appears on the cooled walls of the cell. Nucleation is of minor importance and a growth rate can be imposed by controlling the heat flux (positive temperature gradient in the solid, from the solid to the liquid and in the liquid). The attraction of such approaches lies in the fact that constant growth rate and temperature gradients let us study phenomena like solute rejection ahead of an ice front or particle entrapment by an advancing solid/liquid interface.

Our experimental cell is a vertical cylinder (height 5 mm, diameter $2r_e = 7.5$ mm) bored in a 30-mm copper cube (Fig. 2); the cylinder diameter was chosen for optimal visualization conditions. Its bottom section is closed by a Plexiglas disc that transmits light from the lower part of the cube to the camera. Four K-type 80 μm-diameter microthermocouples are located between the wall and the cell's central axis (at $r = r_e$, $2r_e/3$, $r_e/3$ and $r = 0$), 3 mm above the Plexiglas disc. The thermocouples' reference solders are kept in a thermally stable box which temperature is measured by a PT100 platinum sensor. The minimal delay between two temperature recordings is 0.25 s (≈4 Hz).

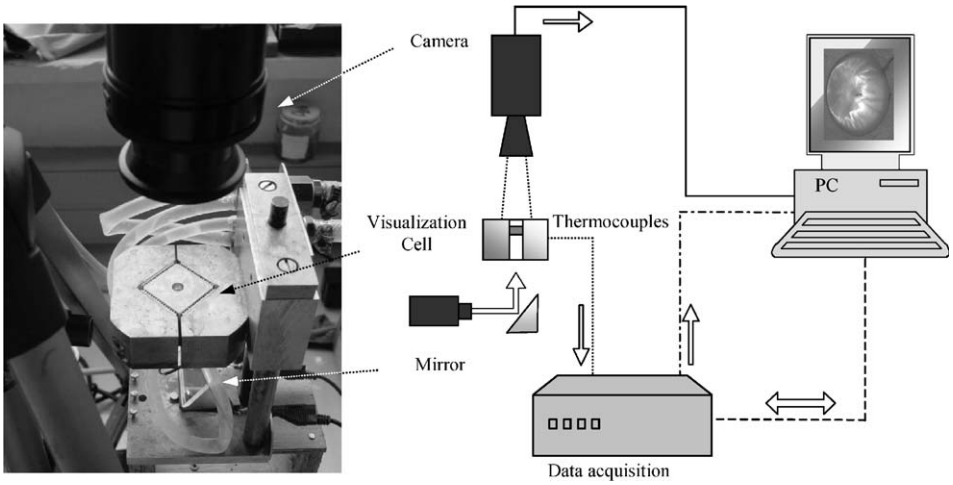

Fig. 2. Experimental set-up: visualization cell and schematic diagram of the acquisition loop.

During tests carried out with water, temperature increases of more than 10 °C between two recordings were properly recorded, showing that this 0.25 s delay is greater than the response time of the 80 μm micro-thermocouples. Measurements carried out during temperature plateau of solidifying (distilled) water showed that the accuracy of the temperature measurements is about ±0.03 °C. The copper cube is cooled by means of four thermoelectric Peltier elements that reject heat toward two water-cooled metal holders. The total surface of the Peltier elements is 144 cm^2. The electrical power is about 100 W, which, depending on the cell temperature, provides cooling power below 1 W in the sample. Thus, the cooling rate of the sample is no more than −0.5 °C/s near the wall. Parameters such as growth rate or temperature gradients are not controlled, unlike in directional growth studies. However, our experimental device differs from those currently used in free crystal growth [3] studies since the sample temperature is not strictly uniform before freezing and the dendrites cannot grow in all directions. Our experimental apparatus thus allows the study of dendrite free growth rate in a particular direction: from cylinder walls to centre. Nucleation inside the sample was never observed.

Fig. 2 is a simplified diagram of the whole experimental facility. A data recording and processing system (acquisition module linked to a computer) is used to analyse temperature evolution as a function of time. Photographs are taken by a high-speed digital camera (77 Hz) linked to the same computer by an acquisition card. Photograph frequency depends on the experiment: since dendrite growth is faster at low antifreeze concentrations, a higher recording frequency is required. The time needed by the dendrites to occupy the whole cell varied between 0.15 s (with 5 wt% of MPG) and about 30 s (with 25 wt% of MPG). The minimum value being lower than the delay between two recordings (0.25 s), temperature measurements cannot provide reliable information about dendrite growth kinetics, especially at low solute concentration. A careful calibration of the photograph frequency allows determination of the dendrite growth rate. The uncertainty in locating the mushy region interface is estimated to about ±0.08 mm. The first picture is triggered by a signal sent by the temperature acquisition module when the wall temperature goes below a threshold value (0 °C in most cases). Precise knowledge of the elapsed time between consecutive photographs also permits correlation with temperature data and thus gives information about the phenomena occurring after the steep temperature rise induced by dendrite growth.

All samples were prepared with pure MPG and demineralised water to prevent heterogeneous nucleation. The three antifreeze concentrations that were chosen for experiments (5, 15 and 25 wt%) correspond to industrial application of ice slurries. Crystallisation was induced mostly by nucleation of water near the thermocouple at the wall. Consequently, the degree of undercooling was not imposed. However, a high number of experiments were carried out in order to increase the undercooling range as much as possible.

4. Dendritic growth front and interdendritic partial solidification front

The return to thermodynamic equilibrium of undercooled liquids is characterised by the fast growth of dendritic crystals. This phenomenon is often followed by the slower propagation of a second ice front corresponding to the continuous sample cooling through the vessel wall. The first interface, here called ''dendritic front'' can be associated with the temperature rise in Fig. 1 (between points *c* and *d*). The second front corresponds to partial solidification of residual liquid entrapped between the dentrites. It also corresponds to the end of the temperature plateau (point *e* in Fig. 1): after the passage of this front, sensible heat again predominates over latent heat. The interest of the experimental cell lies in the fact that it makes possible the association of sample temperature changes with the growth of ice fronts.

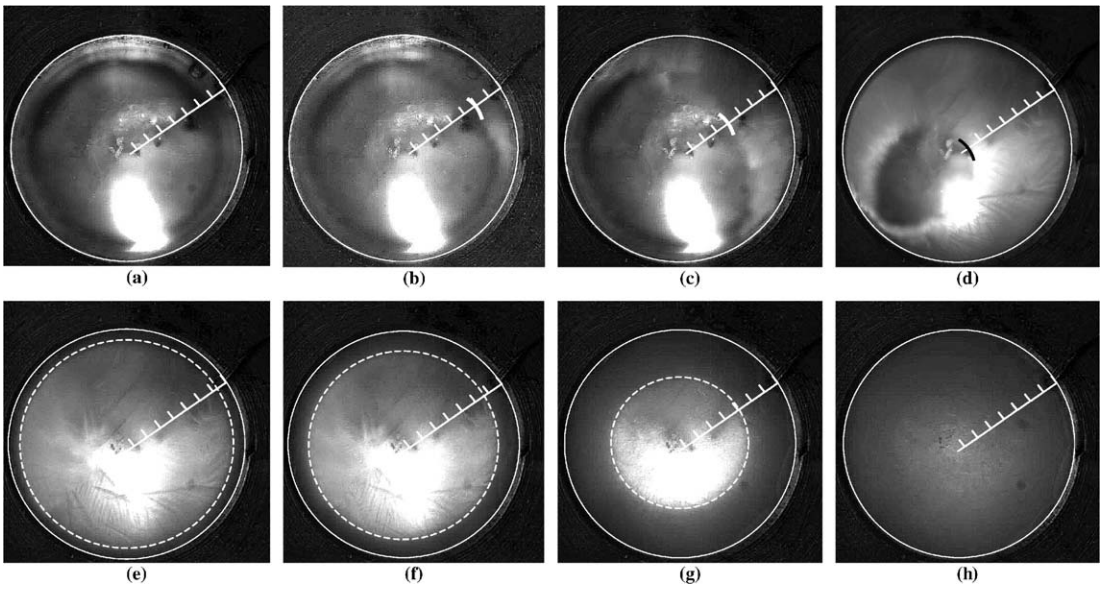

Fig. 3. Growth of the dendritic front and of the interdendritic solidification front in a 5% MPG–water sample: (a) $t_r = 0$ s; (b) $t_r = 0.26$ s; (c) $t_r = 0.65$ s; (d) $t_r = 1.43$ s; (e) $t_r = 2.21$ s; (f) $t_r = 3.26$ s; (g) $t_r = 18.6$ s; (h) $t_r = 52.4$ s.

Fig. 3(a)–(h) are photographs of the entire solidification process in a 5 wt% MPG solution. The phenomena observed with other concentrations recur but the velocity of the dendritic front differs (Section 5). The graduated line allows positioning the ice fronts in Fig. 3(a)–(d). The thick arc marks the location of the dentritic front. The relative time t_r is defined as the time following the appearance of the first crystals ($t_r = 0$ s when the first crystals appear on the wall). The dendrites appear on the wall (where there are privileged sites for nucleation and where the temperature is the lowest) and grow in two directions: from the wall to the cell centre, corresponding to the initial temperature gradient, and along the wall. Thus, the growth of the dendritic front is not axisymmetric and does not end at the centre of the cell. In this particular case, the duration of dendritic growth in the whole 5% MPG sample is less than 2.2 s.

The dotted white circle in Fig. 3(e)–(g) marks the location of the second solidification front corresponding to partial interdentritic solidification. It can be seen that this second front grows uniformly from the wall to the cylinder centre, where it stops after 50 s. This time depends on heat flux at the wall, which can be considered as uniform because of copper's high thermal diffusivity. Fig. 4 shows the progression of ice fronts and the temperature evolutions as functions of time. The circles mark the time at which the location of the second solidification front corresponds to that of the thermocouples ($y = 100\%$, 66%, 33% and 0% on the right-hand vertical axis; with $y(t_r) = 100(r_e - r(t_r))/r_e$). Both the dendritic and interdendritic fronts begin to grow immediately at the wall when $t_r = 0$. Consequently, $y(0) = 0\%$.

4.1. Dendrite growth front

Before $t_r = 0$ s, the sample remains liquid in an undercooled state, the difference between the wall and centre temperatures (almost 3 K) depending on heat flux. Then, the four temperatures rise abruptly to the value corresponding to liquid–solid equilibrium (here $T_{eq} = -1.44$ °C, corresponding to 9 wt% ice in the mixture and 5.6 wt%

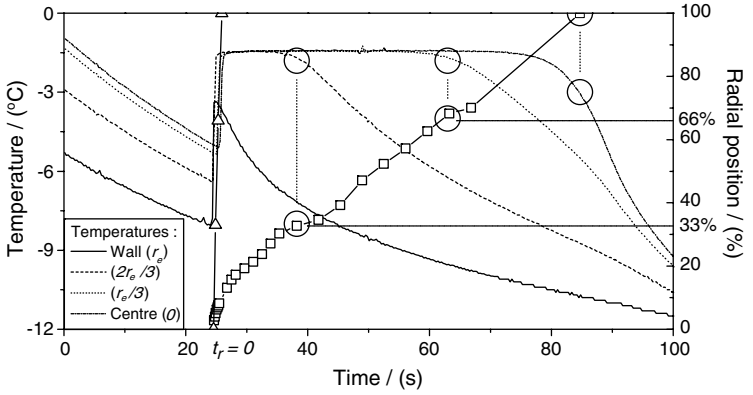

Fig. 4. Progression of the dendritic front (-△-) and the interdendritic solidification front (-□-) and temperature evolution (5% MPG – $T_{eq} = -1.28$ °C).

MPG in the remaining liquid, while the equilibrium temperature of the initial 5 wt% MPG–water mixture is −1.28 °C). Fig. 4 clearly indicates that this temperature increase is associated with the development of dendrites in the whole sample: the maximum delay between the passage of the dendritic front and the recording of the temperature rise never exceeds 0.3 s (the duration of dendritic growth in the whole 5 wt% MPG sample is of about 1.9 s according to the photographic recording and of about 2.5 s according to the temperature recording). This delay is negligible compared to the duration of the solidification plateau (between 15 and 60 s). Finally, we emphasise that the thermocouples are positioned at the middle height of the cell: the simultaneity of temperature rise and crystallisation proves that the growth of the dendrites takes place not only at the free surface but throughout the sample.

4.2. Interdendritic front

Fig. 4 shows that the passage of the second solidification front corresponds to the end of the temperature plateau for all thermocouples. Thereafter, the temperatures decrease more rapidly, indicating that the rate of ice formation and the sample apparent heat capacity are low. The interdendritic front growth rate is linked to many factors, amongst which the antifreeze concentration and the cooling flux predominate: the solution is only partially frozen during the dendritic growth phase and the excess MPG-rich liquid is trapped into the ice matrix; then the freezing of the remaining water consolidates the dendritic structure of the mushy region. As mentioned by Pruppacher [23], this process is much slower (up to several orders of magnitude) than the dendritic growth rate in the case of pure water. The growth of the interdentritic front is always axisymmetric, unlike that of the first front. According to Neilson and Incropera [21], who studied solidification of a binary Na_2CO_3 water solution in a horizontal cylinder annulus, this means probably that conduction is the primary mechanism for heat transfer between the wall and the interdendritic solidification front, the sample composition remaining homogeneous.

4.3. Temperature distributions

Fig. 5 presents the temperature distributions in the 5% MPG solution when the dendritic front ($t_r = 0.9$ s) and the second interdendritic front ($t_r = 38.2$ s) are located between $r = r_e/3$ and $r = 2r_e/3$. One can see that the temperature gradient in the undercooled liquid ahead of the dendritic front is negative (from the wall to the centre), while it is positive in the sample as a whole as the interdendritic front progresses.

5. Dendritic growth rate

5.1. Influence of antifreeze concentration

Fig. 6(a)–(d) were recorded during the growth of the dendritic front in a sample containing 15 wt% MPG;

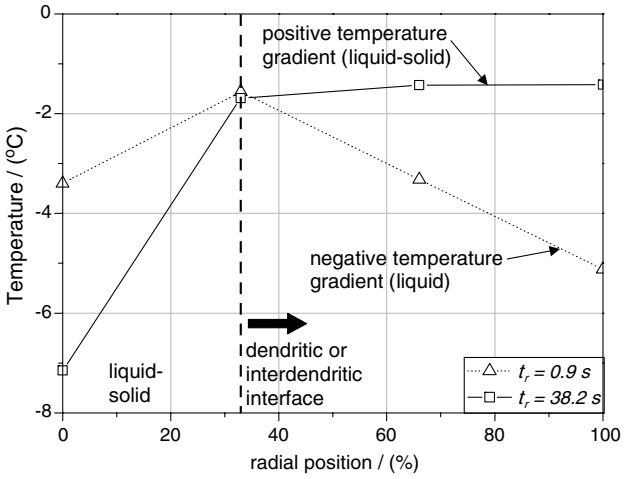

Fig. 5. Temperature distributions in the sample (5% MPG – $T_{eq} = -1.28$ °C) when the dendritic front ($t_r = 0.9$ s) and the interdendritic front ($t_r = 38.2$ s) are between $r = r_e/3$ and $r = 2r_e/3$. The bold dotted line represents the position of the liquidus and the interdendritic interfaces for $t_r = 0.9$ s and $t_r = 38.2$ s, respectively.

Fig. 6(e) shows the corresponding temperature curves. The time needed by the dendrites to reach the cell center is of about 9 s (Fig. 6(d)), whereas it is of about 2 s for samples containing 5 wt% MPG. Note that the delay between the appearance of the first crystals at the wall ($t_r = 0$) and the temperature rise at the cell centre is only of about 4 s: the increase in temperature observed at the cell centre is a consequence of heat diffusion rather than local water crystallisation. When the initial MPG concentration is 25%, only one front is observed: the dendritic growth is low, so that the characteristic times of crystallisation kinetics and of heat diffusion becomes similar.

Two reasons can be adduced for this decrease in dendrite growth kinetics: on the one hand, the migration of water molecules toward the crystals is slowed by the presence of antifreeze; on the other, the increase in antifreeze concentration in the remaining liquid reduces its equilibrium temperature and hence the driving force controlling crystal growth $T_{eq}(x_{a,l}) - T_l$.

5.2. Dendritic growth rate as a function of undercooling degree

Measurements of the dendritic front velocity were performed in the vicinity of each thermocouple in order to derive the relation of the dendritic growth rate to the undercooling degree ΔT (1) and the antifreeze concentration. The velocity of the ice fronts is obtained by a simple derivation of its position with respect to time in the main direction of propagation (radial). However, the first crystals that appear at the wall are not necessarily close to the thermocouple positioned at $r = r_e$ and the volume in which the dendrites grow is strongly reduced near the cell centre ($r = 0$), which could modify their velocity: consequently, only the measurements carried out near the thermocouples at $r = 2r_e/3$ and $r = r_e/3$ are considered.

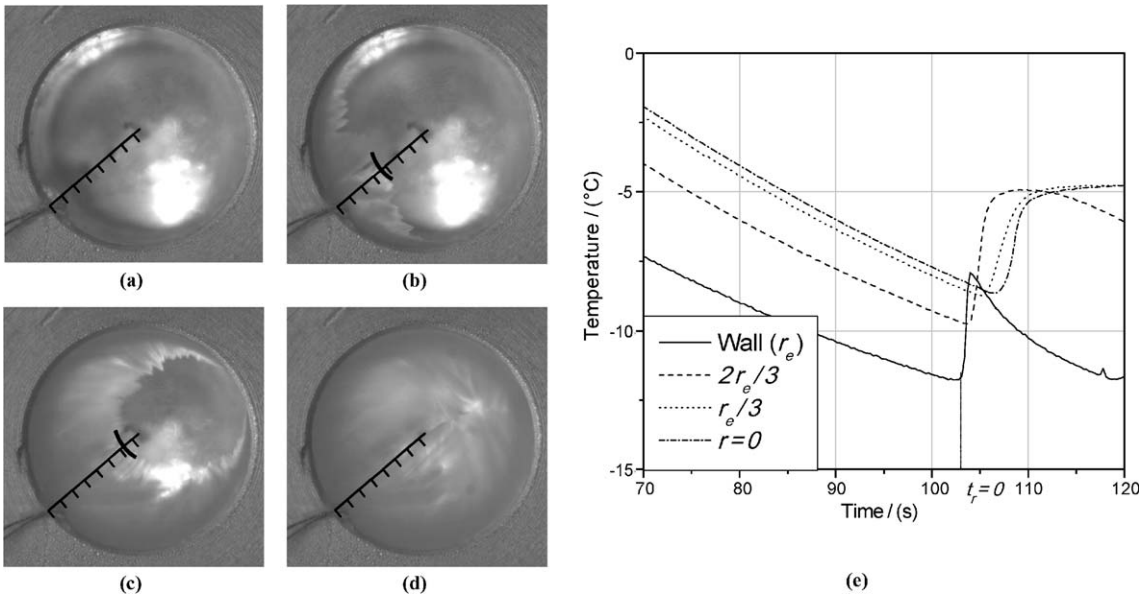

Fig. 6. Progression of the dendritic front in a 15% MPG–water solution ($T_{eq} = -4.49$°C): (a) $t_r = 0$ s; (b) $t_r = 3.03$ s; (c) $t_r = 6.10$ s; (d) $t_r = 9.10$ s; (e) temperature evolution.

Experiments were carried out with aqueous solutions containing 5, 15 and 25 wt% monopropylene glycol (MPG); 25, 30 and 20 cooling cycles were performed, respectively. Each sample was cooled only once.

Fig. 7 confirms that the dendritic growth rate v in the cylindrical cell decreases strongly with the amount of antifreeze in the mixture. It also indicates that the dendritic growth rate seems to increase linearly with the degree of undercooling for antifreeze mass fractions equal to 5 and 15 wt%. Correlations (4) and (5) are merely representative of the crystal growth kinetics of MPG–water solutions in small cylindrical cells

$$v_{x_{a,i}=0.05} = 0.55\Delta T \text{ (Correlation coefficient: 0.79)} \quad (4)$$

$$v_{x_{a,i}=0.15} = 0.12\Delta T \text{ (Correlation coefficient: 0.41)} \quad (5)$$

As discussed above (Section 5.1), one cannot consider the experimental results obtained with the samples containing 25 wt% MPG as representative only of the free crystal growth kinetics. However, it is interesting to note that the growth rate of the solidification front increases slightly with degree of undercooling (whereas the cooling flux remains the same). This indicates that, although crystal growth kinetics is coupled with heat diffusion, it probably remains the limiting factor.

Fig. 8 compares our results to those of Teraoka et al. [18] on the multidirectional free growth of dendrites. Teraoka et al. induced crystallisation at the tip of a capillary tube plunged in a solution of 5 wt% monoethylene glycol (MEG). One can see that the order of magnitude of the dendrite growth rate v is the same in both cases. The results

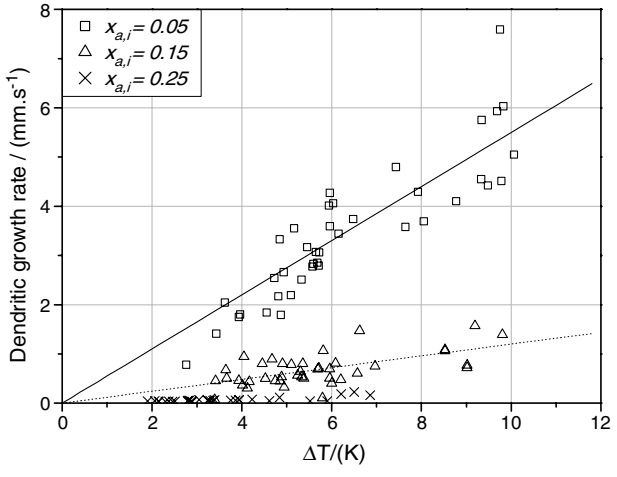

Fig. 7. Dendritic growth rate as a function of undercooling degree ΔT.

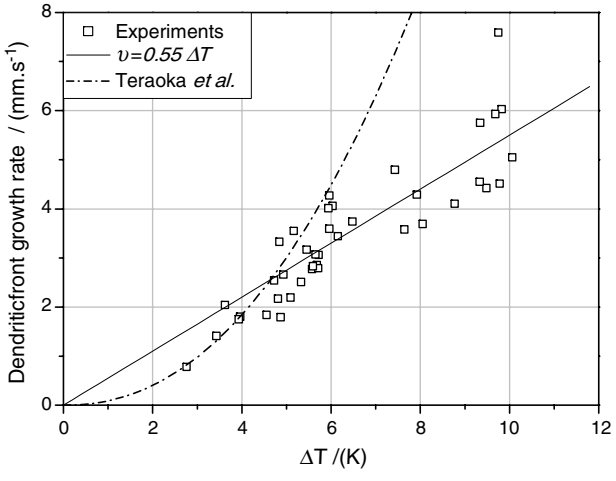

Fig. 8. Dendritic growth rate as a function of undercooling degree ΔT—comparison with Teraoka correlation (5% MPG–water solution).

seem to converge for the smallest degrees of undercooling ($\Delta T < 6$ °C); however, Teraoka et al. described their results by a power law ($v_{x_{a,i}=0.05} = 0.087\Delta T^{2.2}$), whereas the influence of the degree of undercooling on dendritic growth rate is clearly linear in our case. The difference in experimental cell geometry is the most probable explanation for these behaviours.

6. Conclusion

Our experimental set-up lets us study the kinetics of crystallisation in small volumes of undercooled water–antifreeze mixture. When the antifreeze mass fraction is below 25 wt%, the crystallisation process is clearly divided into two stages: dendrite growth and the passage of the interdendritic solidification front. Dendrite growth in the undercooled mixture induces a sudden rise in temperature, while the passage of the interdendritic solidification front determines the time when sensible heat effects again predominate. The experimental results show that the dendrite growth rate is an increasing function of the degree of undercooling and a decreasing function of antifreeze mass fraction. When the antifreeze mass fraction reaches 25 wt%, dendrite growth is so slow that their progress cannot be distinguished from that of the interdendritic solidification front. However, the results suggest that crystallisation kinetics remains the limiting phenomenon.

We plan to carry out similar studies to investigate the importance of geometry and the influence of the solute used on crystallisation kinetics.

References

[1] M. Akyurt, G. Zaki, B. Habeebullah, Freezing phenomena in ice-water systems, Energy Convers. Manage. 43 (2002) 1773–1789.
[2] Y. Kozawa, N. Aizawa, M. Tanino, Study on ice storing characteristics in dynamic-type ice storage system by using supercooled water: effects of the supplying conditions of ice-slurry at deployment to district heating and cooling system, Int. J. Refriger. 28 (2005) 73–82.
[3] H. Müller-Krumbhaar, W. Kurz, Material Science and Technology, in: R.W. Cahn, P. Haasen, E.J. Kramer (Eds.), Phase Transformations in Materials, Part. 10: Solidification, vol. 5, VCH, 1995, pp. 553–632.
[4] P. Papon, J. Leblond, P.H.E. Meijer, Physique des Transitions de Phase: Concepts et Applications, Dunod, Paris, 1999, 390p.
[5] H.P. Huppert, The fluid mechanics of solidification, J. Fluid Mech. 212 (1990) 209–240.
[6] S.L. Chen, P.P. Wang, T.S. Lee, An experimental investigation of nucleation probability of supercooled water inside cylindrical capsules, Exp. Therm. Fluid Sci. 18 (1999) 299–306.
[7] M.S. Christenson, F.P. Incropera, Solidification of an aqueous ammonium chloride in a rectangular cavity—I. Experimental study, Int. J. Heat Mass Transfer 32 (1989) 47–68.
[8] O. Lottin, V. Ayel, H. Peerhossaini, Ice slurries phase transition thermodynamics: relations for determining concentration–temperature domains of application, Int. J. Refriger. 27 (2004) 520–528.
[9] S. Okawa, A. Saito, R. Minami, The solidification phenomenon of the supercooled water containing solid particles, Int. J. Refriger. 24 (2001) 108–117.
[10] S. Okawa, A. Saito, H. Suto, The experimental study on freezing of supercooled water using metallic surface, Int. J. Refriger. 25 (2002) 514–520.
[11] V. Ayel, O. Lottin, E. Popa, H. Peerhossaini, Using undercooling to measure the freezing points of aqueous solutions, Int. J. Therm. Sci. 44 (2005) 11–20.
[12] P.W. Wilson, A.F. Heneghan, A.D.J. Haymet, Ice nucleation in nature: supercooling point (SCP) measurements and the role of heterogeneous nucleation, Cryobioly 46 (2003) 88–98.
[13] C.A. Knight, The Freezing of Supercooled Fluids, D. Van Nostrand, Princeton, NJ, 1967, 145p.
[14] I. Loginova, G. Amberg, J. Ågren, Phase field simulations of non-isothermal binary alloy solidification, Acta Mater. 49 (2001) 573–581.
[15] R.R. Gilpin, The effect of dendritic ice formation in water pipes, Int. J. Heat Mass Transfer 20 (1977) 693–699.
[16] J.S. Langer, Dendrites, viscous fingers and the theory of pattern formation, Science 243 (1989) 1152–1156.
[17] W.W. Mullins, R.F. Sekerka, Morphological stability of a particle growing by diffusion or heat flow, J. Appl. Phys. 34 (1963) 323–329.
[18] Y. Teraoka, A. Saito, S. Okawa, Ice crystal growth in supercooled solution, Int. J. Refriger. 25 (2002) 218–225.
[19] Y. Teraoka, A. Saito, S. Okawa, Study on anisotropy of growth rate of ice crystal in supercooled water, Int. J. Refriger. 27 (2004) 242–247.
[20] H. Schoof, L. Bruns, A. Fischer, I. Heschel, G. Rau, Dendritic ice morphology in unidirectionally solidified collagen suspensions, J. Cryst. Growth 209 (2000) 122–129.
[21] D.G. Neilson, F.P. Incropera, Numerical simulation of solidification in a horizontal cylindrical annulus charged with an aqueous salt solution, Int. J. Heat Mass Transfer 33 (1990) 367–380.
[22] G. Amberg, Parameters ranges in binary solidification from vertical boundaries, Int. J. Heat Mass Transfer 40 (1997) 2565–2578.
[23] H.R. Pruppacher, On the growth of ice crystals in supercooled water and aqueous solution drops, Pure Appl. Geophys. 68 (1967) 186–195.
[24] W.C. Macklin, B.F. Ryan, Growth velocity of ice in supercooled water and aqueous sucrose solutions, Philos. Mag. 17 (1968) 83–87.
[25] K. Ohsaka, E.H. Trinh, Apparatus for measuring the growth velocity of dendritic ice in undercooled water, J. Cryst. Growth 194 (1998) 138–142.